



On the impact of External Pressure on the evolution of Molecular Clouds

Anathpindika, S. V.

*Indian Institute of Technology, Department of Physics,
Kharagpur, West Bengal, India*



Abstract :

Recent observations of Molecular Clouds suggests that ambient environment, i.e., the magnitude of external pressure, affects their evolution. We explored this hypothesis numerically by developing 3-d hydrodynamic realizations of a cloud for different magnitudes of external pressure. It was observed that a cloud experiencing intermediate magnitude of pressure, typically on the order of $\sim 10^4 \text{ K cm}^{-3}$ - 10^5 K cm^{-3} is more propitious for star-formation. We also studied qualitatively the physical processes that lead to this dichotomy.

Introduction :

Fresh analysis of ^{12}CO data from the CfA - Chile survey of Galactic Molecular Clouds supports the earlier hypothesis that ambient conditions in the Galactic disc affect physical properties of clouds (Rice et al. 2016, Heyer et al. 2009). Some of the early work on the subject also showed that size and the turbulent linewidth for clouds were related by a scaling relation of the type, $\sigma \propto L^{0.5}$ (σ is the linewidth and L , the size of a cloud), leading to the inference that clouds were in approximate Virial equilibrium (Solomon et al. 1987). More recent works, however, show that the data are consistent with a more generalised scaling relation of the type, $\sigma \propto \mathbf{b}L^{\mathbf{a}}$, where the coefficients \mathbf{b} and \mathbf{a} vary as a function of the position of a cloud in the Galactic disc (Rice et al.), or vary as a function of the column density of a cloud (Heyer et al.).

Observed variations in the size - linewidth relation has been conceived as evidence supporting the pressure modified Virial equilibrium (PVE), as against the simple Virial equilibrium (SVE). In this scenario, a single value of external pressure is insufficient to reconcile the variation in the size - linewidth relation. Instead, the variation is driven by the difference in magnitude of external pressure ranging between 10^4 K cm^{-3} - 10^8 K cm^{-3} found in various parts of the Galactic disc (Field et al. 2011). Furthermore, the fact that clouds form via turbulent fragmentation in the ISM, the process must necessarily involve a flux of mass, momentum and energy between the cloud and the ISM which also makes it unlikely that clouds will obey the SVE (Ballesteros - Paredes 2006).

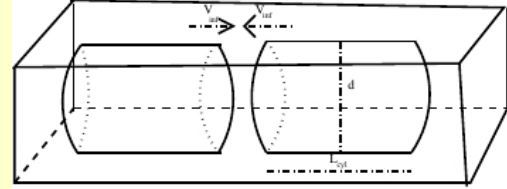
Numerical Method and set - up :

Hydrodynamic models were developed using the **Smoothed Particles Hydrodynamics** code **SEREN**. Each realisation was developed with 2.15 M gas particles and 0.85 M particles representing the externally confining intercloud medium, resulting in mean spatial resolution on the order of ~ 0.1 pc. Sink particles were not used as we were not interested in collating statistical data of prestellar objects. We used adaptive smoothing lengths so that each SPH particle had exactly 50 neighbours. Dynamic cooling of post-collision slab was implemented with the help of the standard cooling curve for the ISM.

We used a relatively simple set - up to assemble a cloud via head-on convergence of identical cylindrical gas flows shown in the cartoon below. Realisations were repeated for different magnitudes of initial in-flow velocity, V_{inf} , length and radius of pre-collision cylinder, respectively L_{cyl} and R_{cyl} , and average initial gas density, \bar{n} . Choice of parameters used in these realizations are listed in the table below.

List of Parameters for models developed

Serial No.	Physical Properties	Pre-collision Velocity of gas-flows, V_{inf} [(km/s)] Pre-collision Mach number (\mathcal{M})	$(\frac{\rho_{gas}}{\rho_H})$ [$K \text{ cm}^{-3}$]	M_{gas} [M_{\odot}]	M_{min}^a [M_{\odot}]	Comment
1	$L_{cyl} = 130 \text{ pc}$, $R_{cyl} = 14 \text{ pc}$ $\bar{n} = 1 \text{ cm}^{-3}$, $T_{gas} = 5000 \text{ K}$ $n_{max} \sim 10^6 \text{ cm}^{-3}$, $n_{avg}^{int} \sim 0.2 \text{ pc}$	4.8 (0.7)	2.8×10^3	4.3×10^3	0.2	Warm Atomic Flow ($\mu = 1 \text{ amu}$)
2	Same as (1)	9.0 (1.4)	9.8×10^3	4.3×10^3	0.2	Warm Atomic Flow
3	Same as (1)	19.28 (3.0)	4.45×10^4	4.3×10^3	0.2	Warm Atomic Flow
4	$L_{cyl} = 50 \text{ pc}$, $R_{cyl} = 10 \text{ pc}$ $\bar{n} = 50 \text{ cm}^{-3}$, $T_{gas} = 500 \text{ K}$ $n_{max} \sim 10^6 \text{ cm}^{-3}$, $n_{avg}^{int} \sim 0.13 \text{ pc}$	3.45 (1.7)	7.3×10^4	4.2×10^4	2.0	Warm Atomic Flow ($\mu = 1 \text{ amu}$)
5	Same as (4)	6.1 (3.0)	2.25×10^5	4.2×10^4	2.0	Warm Atomic Flow
6	Same as (4)	10.36 (5.1)	6.51×10^5	4.2×10^4	2.0	Warm Atomic Flow
7	$L_{cyl} = 30 \text{ pc}$, $R_{cyl} = 10 \text{ pc}$ $\bar{n} = 100 \text{ cm}^{-3}$, $T_{gas} = 40 \text{ K}$ $n_{max} \sim 10^6 \text{ cm}^{-3}$, $n_{avg}^{int} \sim 0.1 \text{ pc}$	5.6 (15.1)	9.0×10^5	1.2×10^5	6.0	Cold Molecular Flow ($\mu = 2.29 \text{ amu}$)
8	Same as (7)	7.43 (20.0)	1.6×10^6	1.2×10^5	6.0	Cold Molecular Flow
9	Same as (7)	14.86 (40.0)	6.4×10^6	1.2×10^5	6.0	Cold Molecular Flow
10	Same as (7)	29.7 (79.97)	2.56×10^7	1.2×10^5	6.0	Cold Molecular Flow
11	Same as (7)	55.6 (149.7)	8.9×10^7	1.2×10^5	6.0	Cold Molecular Flow



Cartoon showing a schematic representation of a head-on collision between identical cylindrical gas-flows. Each flow has length, L_{cyl} , radius, $R_{cyl} = 0.5*d$, and initial velocity magnitude, V_{inf} . See Table 1 for other physical details.

Results :

Evolution of the post-collision slab

Colliding gas-flows assembled a slab at the centre of the computational domain. The ram-pressure confined slab in case of sub-sonic gas-flows evolved via the interplay between the gravitational instability and the thermal instability. By contrast, the shock-confined slab resulting from a collision between super-sonic gas-flows evolved via the interplay between the Thin shell instability (TSI) that soon after being triggered, grows in non-linear fashion, and the thermal instability. Rapid growth of the TSI sheared the layers of gas within the slab and caused it to buckle. [Rendered density image on the upper - panel of **Fig.1(a)** below shows the time evolution of the shocked slab in one of the realisations. On the lower panel of this figure is a cross-section of the same slab showing its copious fragmentation.]

This inter-layer shear dissipated turbulent energy and as a result the slab soon puffed - up and collapsed to the central plane as soon it lost support against self-gravity. [Images in **Fig. 1(b)** show the puffed slab and the end result of such a collapsed slab. Formation of dense filamentary structure in the collapsed slab is clearly visible in the right had panel of this picture.]

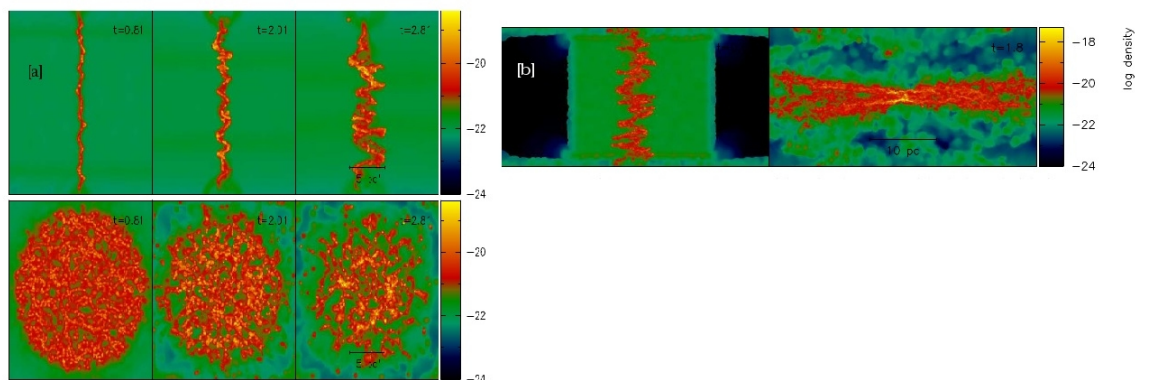


Figure 1

Velocity dispersion, Viral state and the column density PDF as a function of external pressure -

Turbulent velocity in the assembled cloud increases with rising external pressure which is consistent with the analytic prediction of Greenbelt (1989), marked by the continuous emerald line in **Fig. 2[a]**.

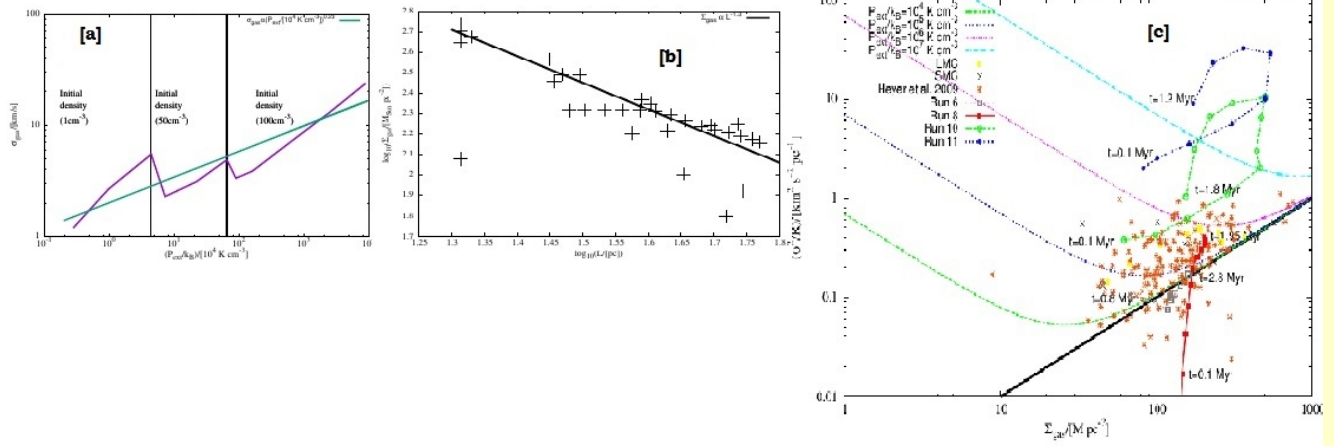


Figure 2

Surface density - size correlation shown in **Fig. 2 [b]** for clouds assembled in these realizations is also significantly steeper than that observed by Larson (1981) for his sample of clouds. **Contrary to the suggestion by Larson (1981), plot in Fig. 2[b] implies that clouds are not entities of uniform surface density.**

Finally, shown in **Fig. 2[c]** is the size line width coefficient as a function of the cloud column density. The black continuous line in this plot corresponds to the SVE while the coloured 'V' - shaped curves represent the PVE for different external pressures. The PVE is given the expression -

$$\frac{\sigma_{gas}^2}{L} = \frac{1}{6} \left(\pi \Gamma G \Sigma_{gas} + \frac{4P_{ext}}{\Sigma_{gas}} \right)$$

The SVE is recovered from this expression by setting the P_{ext} term in it to zero. Evidently, observational data for various clouds and indeed, data for the clouds assembled in these realisations are consistent with the PVE.

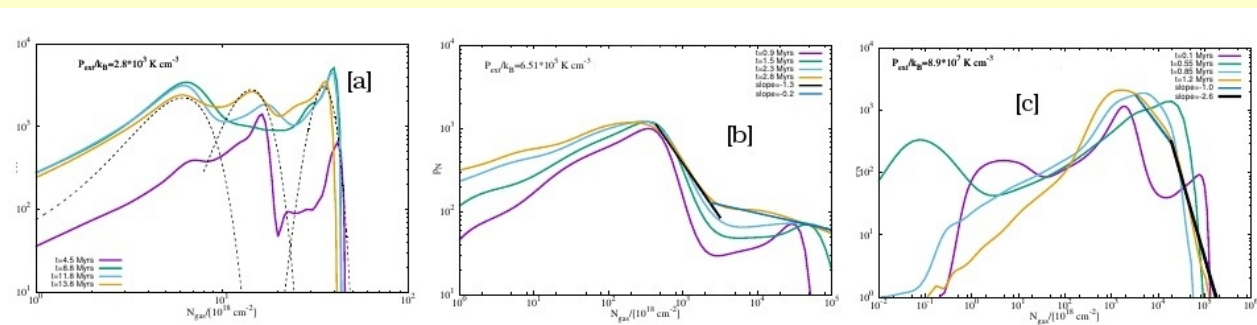


Figure 3

Finally the column density probability distribution function (NPDF) for three choices of external pressure can be seen on the respective panels of **Fig. 3**. Observe that only a relatively small fraction of gas is cycled in to the dense putative star-forming phase, i.e., with column density $\geq 10^{21} \text{ cm}^{-2}$, for extreme choices of external pressure [See panels **(a)** and **(c)** above].

In these latter cases [**Fig. 3 (a) and 3 (c)**] the PDF is largely log normal (rather a composition of log normal distributions) with virtually no power-law extension into higher densities. A cloud confined by an intermediate magnitude of pressure, i.e., $\sim 10^5 \text{ K cm}^{-3}$, however, appears most propitious for star-formation which is consistent with observations of local star-forming regions. The NPDF in this case is a composition of a lognormal profile at lower densities followed by a distinct power-law extension into higher densities.

Conclusions :

External pressure bears upon the physical properties of Molecular clouds. Apparently clouds do not exhibit a unique set of properties, but rather a bouquet of properties modulated by the ambient environment. Star - formation appears to be inhibited in low pressure environment as well as in extreme environment where the external pressure is significantly large. Intermediate pressure $\sim 10^5 \text{ K cm}^{-3}$ appears favourable for stars to form.

This finding is consistent with the fact that clouds in the Solar neighborhood - where the external pressure is $\sim 10^5 \text{ K cm}^{-3}$ - generally form stars more efficiently than those at the periphery of the Galactic disk (where the pressure is much lower), or indeed, close to the Galactic centre (where the pressure is significantly higher).

At large external pressure, typically $\geq 10^7 \text{ K cm}^{-3}$, the post-collision slab is attended to by the shell instability that quickly subverts the gravitational instability. Growth of the TSI and its non-linear excursion dissipates the turbulent support of the slab and causes it to collapse to its central plane without ever cycling much gas into the dense, putative star-forming phase. At small pressures, typically $\leq 10^4 \text{ K cm}^{-3}$, much of the gas remains warm and therefore atomic (i.e., remains at significantly low densities) which effectively stymies star-formation.

Our results show that clouds are unlikely to be virialised entities as is often believed to be the case. At best, clouds may obey the pressure modified Virial equilibrium. This result has profound implications for the theory of star-formation, for it is based on the assumption of clouds being Virialised entities and that the efficiency of star-formation is modulated only by the turbulent Mach number and the Virial parameter for a cloud.

References :

- (a) Anathpindika, S., Burkert, A & Kuiper, R., MNRAS, 2017, 466, 4633
- (b) Rice, T., Goodman, A., Bergin, E., Beumont, C & Dame, T., 2016, ApJ, 822, 52
- (c) Heyer, M., Krawczyk, C., Duval, J & Jackson, J., 2009, ApJ, 699, 1092
- (d) Ballesteros - Paredes, J., 2006, MNRAS, 372, 443
- (e) Elmegreen, B., 1989, ApJ, 338, 178
- (f) Solomon, P., Rivolo, A. R., Barrett, J & Yahil, A., 1987, ApJ, 319, 730
- (g) Larson, R., 1981, MNRAS, 194, 809

Acknowledgments :

This work was supported by the Science & Engineering Research Board (SERB) of the Department of Science & Technology, Govt of India, via the grant No. YES/00304/2014 under the Young Scientist Scheme. The author is also indebted to the Royal Astronomical Society for its bursary that permitted him to visit the Department of Astronomy & Astrophysics, University of Tübingen, and the Ludwig Maximilian University, Muenich, where this project was conceived. Simulations in this work were developed on the bwGRiD computing cluster, a member of the German D-Grid initiative, funded by the Ministry for Education and Research (Bundesministerium für Bildung und Forschung) and the Ministry for Science, Research and Arts Baden-Württemberg (Ministerium für Wissenschaft, Forschung und Kunst Baden-Württemberg).